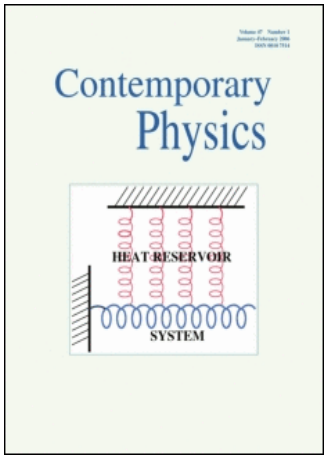

Contemporary Physics
Publication details, including instructions for authors and subscription information:
http://www.informaworld.com/smpp/title~content=t713394025

Detecting quantum light

Christine Silberhorn [a]
[a] Max-Planck Research Group, IOIP, Erlangen, Germany

Online Publication Date: 01 May 2007
To cite this Article: Silberhorn, Christine (2007) 'Detecting quantum light', Contemporary Physics, 48:3, 143 - 156
To link to this article: DOI: 10.1080/00107510701662538
URL: http://dx.doi.org/10.1080/00107510701662538

Contemporary Physics, Vol. 48, No. 3, May–June 2007, 143–156

Taylor & Francis
Taylor & Francis Group

Detecting quantum light

CHRISTINE SILBERHORN*

Max-Planck Research Group, IOIP, Günther Scharowsky-Str. 1/Bau 24, 91058 Erlangen, Germany

(*Received 30 July 2007; in final form 20 August 2007*)

The quantization of light is the basis for quantum optics and has led to the observation of a multitude of genuine quantum effects which cannot be explained by classical physics. Yet, there exist different views when we refer to the distinct quantum character of light as opposed to classical fields. A major impact on how we describe photonic states is caused by the detection method we use for the quantum state characterization. In the theoretical modelling measuring light always means the recording of photon statistics of some kind, though the way we interpret the results is quite different and depends mainly on the intensity of actual detected light. If we use conventional photodiodes and monitor bright light, we attribute the detected statistics to quadrature measurements in a phase space representation, or—in other words—we identify the quantum state by studying its uncertainties of its field amplitude and phase properties which correspond to conjugate quantum observables. For multi-photon states with very low intensity we have to employ avalanche photodiodes (APDs) to be able to see any signal, but photon number resolution seems difficult in this regime. Recent developments allow one to ascertain information about the photon statistics from APD measurements opening up new routes for characterizing photonic states. In this article we review the different methods for modern quantum state metrology where we include theoretical aspects as well as the description of the state-of-the-art technology for measuring photon statistics.

1. Introduction

The observation of light has a long history which has led to surprising insights in our understanding of modern physics. Classical optics describes light propagation and its interaction with matter as waves which can exhibit different optical frequencies, polarizations and wave propagation vectors. As an underlying principle we interpret light waves as coherent electromagnetic radiation with defined electric and magnetic field vectors. The propagation behaviour of the associated fields can be derived from Maxwell's equations which have been extremely successful in explaining the observations of a manifold of interference and diffraction experiments. Thus, at the beginning of the last century most scientists believed in the wave nature of light and considered research in optics as being completed in terms of fundamental physics.

Yet, one phenomena remained where physicists puzzled to find a good agreement between their theory and experimental results: studying the spectral intensity distribution of black-body radiation it appeared impossible to come up with one single formula which was valid for the high and low frequency range. In 1900 Max Planck succeeded in deriving an appropriate black-body radiation law by proposing the idea that light could only be emitted in discrete energy portions. Whereas Max Planck himself was convinced that his assumption had a purely formal background, his invention has actually led to the

*Corresponding author. Email: csilberhorn@optik.uni-erlangen.de

Contemporary Physics
ISSN 0010-7514 print/ISSN 1366-5812 online © 2007 Taylor & Francis
http://www.tandf.co.uk/journals
DOI: 10.1080/00107510701662538

development of the theory of quantum mechanics. During the same time in 1902 Lenard conducted an experiment investigating the energy of electrons generated by the illumination of a metal surface. Today we know his results as the photoelectric effect, which again appears difficult to describe by the absorption of light wave radiation. It was Einstein, who proposed in the year 1905 the quantization the light field and called one energy quant of light a photon. His theory could explain both Max Plancks laws and the photoelectric effect; it was the starting point for a new research discipline: quantum optics.

Lenard's experiment also already illustrated that light can cause an electric current in response to the flow of photons impinging on a photoemissive cathode. The released photons are denoted as photo-electrons. Devices monitoring the optical fields by this principle have become one of the most important instruments in light applications, known as photoelectric detectors.

2. Quantum light

Quantum optics investigates distinct properties of light, which reflect the quantum character of the light. By introducing the field quantization light is considered to exhibit simultaneously both wave and particle properties. Depending on the experimental arrangements and our information about the system, our observations of light phenomena highlight either the coherence of the fields or the graining of the energy. Research in quantum optics in the last century has been extremely successful and has given rise to the development of novel technologies, most prominently the invention of the laser. In addition, it also stimulated theoretical studies of fundamental aspects of our understanding of quantum physics. The importance and topicality of this area can be seen by the award of several Nobel prizes during the last decades. In 2005, Roy Glauber received the Nobel prize for research where the committee recognized 'his contribution to quantum theory of optical coherence'. The theory of optical coherence investigates the properties of light in terms of correlation functions between two distinct fields or of a single field at different points in time and space. Laser light is characterized by extraordinary small fluctuations in its field amplitude, which implies that it exhibits extremely long coherence lengths. Thus, in classical optics we consider laser light as ideal monochromatic waves with constant electromagnetic field amplitudes which allow for high contrast interference patterns. In quantum optics laser light is described by coherent states, which are considered as the most 'classical' light since they come closest to our expectations we have from our understanding of light as electromagnetic waves.

The quantum properties of light originate from the quantization of electromagnetic field radiation. A monochromatic mode of an optical field with frequency ω and wave vector $\mathbf{k}$ can be represented classically as a harmonic oscillation[†]

$$\mathbf{E}(\mathbf{r},t) \propto A\,\exp\left[-\mathrm{i}(\omega t-\mathbf{k}\cdot\mathbf{r})\right]+A^{*}\exp\left[\mathrm{i}(\omega t-\mathbf{k}\cdot\mathbf{r})\right],$$

where $A \in \mathbb{C}$ is defined as the complex field amplitude. Alternatively, we may use a completely real description

$$\mathbf{E}(\mathbf{r},t) \propto X\cos\left(\omega t-\mathbf{k}\cdot\mathbf{r}\right)+Y\sin\left(\omega t-\mathbf{k}\cdot\mathbf{r}\right)$$

and define the quadratures X and Y as the real and imaginary part of A.

We introduce the quantization of light by interpreting the monochromatic optical mode as a quantum harmonic oscillator, which exhibits discrete energy levels. For quantum states of light we call these energy levels photons, i.e. one field containing one, two or three photons exhibits energies corresponding to the first, second or third excitation. The formal analogy between the quantum mechanical harmonic oscillator and the oscillation of the field modes allows us to associate the following quantum operators to the classical parameters:

$$\hat{a}\leftrightarrow A,\quad \hat{a}^{\dagger}\leftrightarrow A^{*},\qquad \hat{x}\leftrightarrow X,\quad \hat{p}\leftrightarrow Y.$$

Hereby, the operators $\hat{a}$, $\hat{a}^{\dagger}$ denote the ladder operators of the quantum oscillator and are interpreted for optical field modes as photon creation and annihilation operators. The operators $\hat{x}$ and $\hat{p}$ correspond to the position and momentum of a quantum harmonic oscillator, which are known to fulfill the Heisenberg uncertainty relationship as non-commuting variables. Accordingly for photonic states the two orthogonal quadrature components[‡] $\hat{X}=\hat{a}+\hat{a}^{\dagger}$, $\hat{Y}=-\mathrm{i}(\hat{a}-\hat{a}^{\dagger})$ define a pair of non-conjugate variables which can never be determined simultaneously with absolute accuracy. More generally we can define the quadrature operator

$$\hat{X}_{\phi}=\hat{a}\,\exp\left(-\mathrm{i}\phi\right)+\hat{a}^{\dagger}\,\exp\left(\mathrm{i}\phi\right)$$

describing the quadrature $\hat{X}_{\phi}$, which is rotated relative to $\hat{X}$ by the angle ϕ.

Coherent light with classical field amplitude α corresponds to a quantum state with minimal uncertainty with symmetric distribution in the quadrature components, such that

$$\left\langle\alpha\middle|\Delta^{2}\hat{X}_{\phi}\middle|\alpha\right\rangle=\left\langle\alpha\middle|\Delta^{2}\hat{X}_{\phi+\pi/2}\middle|\alpha\right\rangle\quad\text{for all }\phi\in\mathbb{R}.$$

†Note, that these definitions assume implicitly a global reference phase; different reference phases correspond to rotated coordinate systems in the phase space representation.

‡For simplicity we neglect normalization factors.

Describing the coherent field mode formally as quantum state $|\alpha\rangle$ we obtain

$$|\alpha\rangle = \exp(\alpha\hat{a}^\dagger - \alpha^*\hat{a})|0\rangle,$$

with $|0\rangle$ being the ground state of the optical mode. The operator $D(\hat{\alpha}) = \exp(\alpha\hat{a}^\dagger - \alpha^*\hat{a})$ characterizes a displacement of the vacuum state $|0\rangle$ in the phase space (see below) according to the classical field amplitude α. Furthermore, it is easy to show that coherent states are eigenstates of the annihilation operator $\hat{a}$ with eigenvalue α, i.e $\hat{a}|\alpha\rangle = \alpha|\alpha\rangle$. Expanding coherent states in the photon number basis we obtain

$$|\alpha\rangle = \exp\left(-\frac{|\alpha|^2}{2}\right)\sum_n \frac{\alpha^n}{(n!)^{1/2}}|n\rangle.$$

The associated probability distributions are known from mathematics as Poissonian distribution, which are typical for the statistics of random processes (see figure 1).

For arbitrary quantum states of light we can assign two different descriptions. They provide both a complete characterization of the state, but highlight different properties of the light. The particle nature of the light corresponds to the observation of photon number statistics. A pure state can be defined in the photon number basis as

$$|\Psi\rangle = \sum_n c_n|n\rangle, \quad c_n \in \mathbb{C},$$

whereas more generally every mixed state can be represented by

$$\hat{\rho} = \sum_{m,n} c_{mn}|m\rangle\langle n|, \quad c_{mn} \in \mathbb{C}.$$

The quantumness is reflected by the discreteness of the allowed energies and shows up in measurements of photon statistics.

Alternatively we may characterize a photonic state in a phase space representation which is closer related to the wave nature of light. In a classical picture a coherent optical mode can be represented by its complex field amplitude in a phase space where the quadratures X and Y serve as the coordinate axes. Remember, that the quantum quadratures $\hat{X}$ and $\hat{Y}$ are conjugate variables and thus cannot be simultaneously be well defined in the quantum phase space. For this reason the generalization of the classical phase space into an appropriate quantum representation is not straightforward. There actually exist different types of quasi-probability distributions defining quantum phase space representations. These distributions all relate the probabilities of measurement outcomes to the formal description of the states. But since single points are ill-defined they can become singular or even negative. The representations distinguish each other by different definition of the meaning of one point in phase space. The Glauber–Sudarshan P-representation interprets every point as a coherent state and the respective density matrix is then given by [1]

$$\hat{\rho} = \int P(\alpha)|\alpha\rangle\langle\alpha|,$$

where $P(\alpha)$ denotes the quasi-probability distributions corresponding to the P-representation. In this representation the coherent states serve as a basis for the state characterization, but due to the over-completeness† of the set of coherent states $P(\alpha)$ the P-functions become singular and/or negative for many quantum states, including the coherent states themselves. Contrariwise, the Husimi Q-function overcomes this problem as it characterizes states by introducing the overlap between the signal state $\hat{\rho}$ and all possible coherent states such that it is defined by

$$Q(\alpha) = \frac{1}{\pi}\langle\alpha|\hat{\rho}|\alpha\rangle.$$

The definition of Wigner functions emphasizes the uncertainty of the quadratures X and Y in phase space and provide the closest link to homodyne measurements (see below). Formally it is described as

$$W(X,Y) = \frac{1}{2\pi}\int_{-\infty}^{\infty}\exp(\mathrm{i}Y\,x)\left\langle X - \frac{x}{2}|\hat{\rho}|X + \frac{x}{2}\right\rangle \mathrm{d}x.$$

Figure 2 depicts the Wigner function of a coherent state in phase space. The quasi-probability distributions of a coherent state corresponds to a Gaussian function where the variances of the quadratures are directly related to the widths of the Gaussian. For a simplified illustration of quantum light we can use cross-sections of Wigner functions to depict the associated quantum light with its uncertainties.

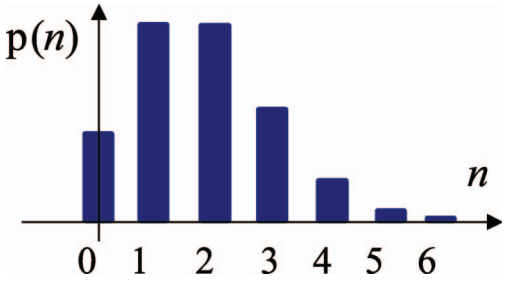

Figure 1. Photon number probabilities of a coherent state; the statistics are given as Poissonian distribution with $\Delta^2 n = n$.

†This means that two coherent states with field amplitudes α and β are actually non-orthogonal to each other $|\langle\alpha||\beta\rangle|^2 = \exp(-|\alpha-\beta|^2)$, but the set of all coherent states fulfills the completeness relationship $(1/\pi)\int|\alpha\rangle\langle\alpha|\mathrm{d}^2\alpha = 1$, which is needed to define a basis set.

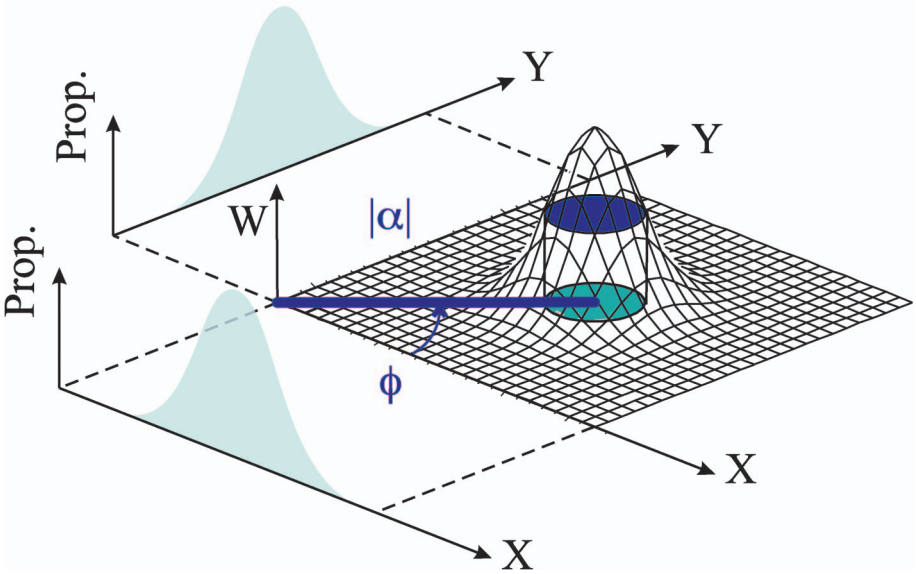

Figure 2. Representation of a coherent state in phase space by its Wigner function. The state has a field amplitude $\alpha = |\alpha| \exp(i\phi)$; the integration over one quadrature yields the probabilities to measure specific values for the conjugate quadrature as indicated in the figure. The corresponding probability distributions are called the marginal quadrature distributions.

We can distinguish quantum properties of light in comparison to coherent states and superpositions of these, which denote as 'classical' light by definition†. In terms of the P-representation we then understand light as non-classical if it exhibits negative contributions. Translating this condition to the photon number statistics they become non-classical if they cannot be described by a mixture of Poissonian probability distributions [1] (see figure 3).

For Wigner functions negative values of the phase space representation clearly indicate the quantum character of the light. Though states which have completely positive Wigner functions are also considered as non-classical if their uncertainty is non-compatible with coherent state mixtures. This is, for example, the case if one of the quadratures has a reduced uncertainty at the expense of its conjugate one. These states are known as so-called quadrature squeezed states (see e.g. [2]; see figure 4). More generally one defines Gaussian states as quantum states which exhibit a Gaussian Wigner function and thus are completely characterized by their first- and second-order moments. They are typically described by a pair of conjugate quadrature operators, and since these exhibit a continuous eigen value spectra the corresponding states are also referred to as continuous variable (CV) states.

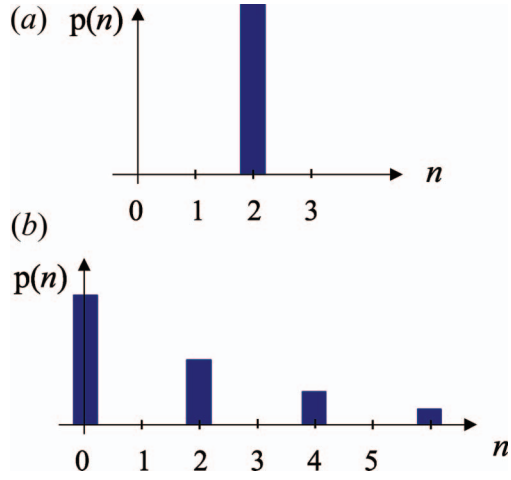

Figure 3. Photon number statistics of non-classical states (see text); (*a*) photon number state and (*b*) single mode squeezed state.

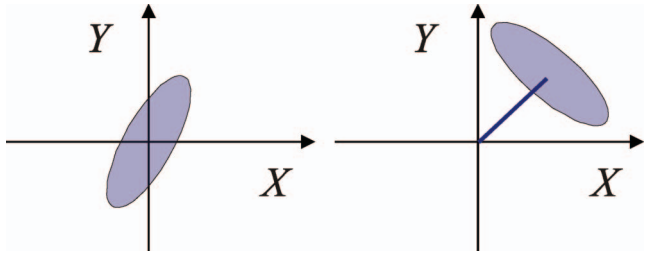

Figure 4. Phase space representation of squeezed states; the uncertainty of one quadrature is reduced at the expense of an enlarged uncertainty in the conjugate quadrature.

†Although this definition suggests that coherent light has no quantum properties, one should keep in mind that in the framework of quantum optics actually all states are quantum states; coherent states do actually exhibit properties which cannot be understood by classical optics.

3. Theory of photo-detection

Photo-detection describes the process of photons being absorbed by some medium and converted into electric charges, which get subsequently detected as photocurrent. In the classical description we relate the generated photocurrent to the time-averaged energy or intensity of the incident light field $\mathbf{E}(\mathbf{r}, t)$

$$I \propto \int \mathrm{d}t |\mathbf{E}(\mathbf{r}, t)|^2 = \langle AA^* \rangle,$$

where A is the defined complex field amplitude. The probability of a photon being absorbed at time t during the time interval Δt can then be defined by

$$p(t) \propto \Delta t \langle I \rangle.$$

If we translate by analogy the classical quantities to its associated quantum operators we find that the probability of photon-absorption is given by

$$i(t) = \frac{\langle p(t) \rangle}{\Delta t} \propto \langle \hat{a}^\dagger \hat{a} \rangle = \langle \hat{N} \rangle.$$

Thus, the averaged resulting photocurrent $i(t)$ is proportional to the flux or number of impinging photons.

In a more precise approach we can understand the process of photon absorption by considering the transition amplitudes of the photon annihilation operator. For a given input state $|in\rangle$ and a basis set of possible output states $\{|out\rangle\}$ we obtain for one specific output state $|out\rangle$ the expression $\langle out|\hat{a}|in\rangle$. To calculate the total transition probability we have to allow for all possible output states and obtain

$$\sum_{out} |\langle out|\hat{a}|in\rangle|^2 = \sum_{out} \langle in|\hat{a}^\dagger|out\rangle\langle out|\hat{a}|in\rangle.$$

With the completeness relation $\sum_{out} |out\rangle\langle out| = \mathbb{1}$ this expression yields the same photon counting probability

$$\langle p(t) \rangle \propto \left\langle in|\hat{a}^\dagger \hat{a}|in \right\rangle = \langle \hat{n} \rangle.$$

For an unknown input state of an ensemble measurement we have to average over all possible input states. In a more formal treatment this is described by introducing mixed states with density operators $\hat{\rho}$ such that the averaged photon counting probability becomes

$$\langle p(t) \rangle = \sum_{in} p_{in} \langle in|\hat{a}^\dagger \hat{a}|in\rangle = \mathrm{tr}(\hat{\rho}\hat{a}^\dagger \hat{a}).$$

In counting experiments we are often not only interested in averaged measurement results—such as the mean value or variance of the photon number distributions—but we also want to predict the probability of one single-shot measurement. Thus, we would like to define measurement operators $\hat{M}_N$ for individual detection events, which fulfill the conditions $|out\rangle \propto \hat{M}_N|in\rangle = |N\rangle$, and the probability $p_n = \langle in|\hat{M}_N|in\rangle$. By rewriting our derived photo-detection operator of ensemble measurements we find

$$\hat{a}^\dagger \hat{a} = \sum_N \hat{a}^\dagger \hat{a}|N\rangle\langle N| = \sum_N N|N\rangle\langle N|.$$

If we associate $\hat{M}_N = |N\rangle\langle N|$ with single-shot measurements of a perfect photon counting detector the measured statistics become consistent with the interpretation of projecting states onto the photon number basis with the probability $\mathrm{tr}(\hat{\rho}|N\rangle\langle N|)$. For the pure state $|in\rangle$ the probability of a N photon detection event takes the familiar form $\langle in|N\rangle\langle N|in\rangle$.

4. Photo-detectors

For standard applications in optical technologies the detection of light is accomplished by photodiodes (see figure 5). These diodes are built from p- and n-doped semiconductor materials where the corresponding bandgap determines the detectable optical wavelengths. At the p–n junction a charge carrier depletion region with a corresponding internal field develops. When light of sufficient photon energy impinges on the diode a mobile electron gets excited and creates an electron–hole pair. Due to the internal field across the depletion region a measurable photocurrent proportional to the number of incident photons is generated.

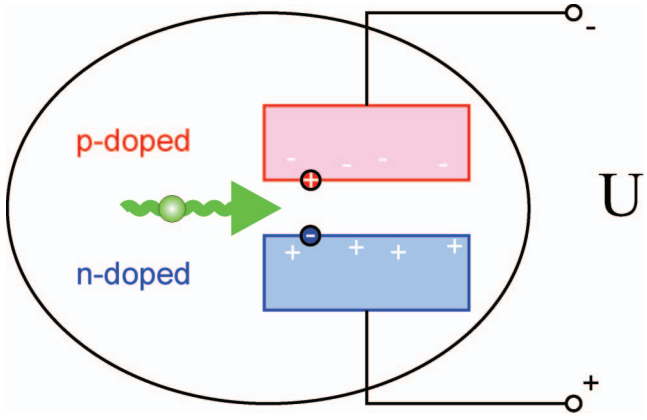

Figure 5. Conventional photodiodes are built from p- and n-doped semiconductor material such that at the interface between these materials a space-charge layer is formed. Every incident photon causes the generation of an electron–hole pair, which can be detected photon current if a voltage U is applied across the diode. Ideally these diodes allow a perfect mapping of the photon statistics to measured currents. However, photodiodes always also show some noise background such that single or few photons cannot be seen.

The performance of photodiodes is characterized by its responsivity, which directly relates to the quantum efficiency, and its noise behaviour specified by the dark current and noise-equivalent power. The quantum efficiency η is defined as the ratio between the detected photons, i.e. created electron–hole pairs, and incident photons. Depending on the wavelengths, respectively, the used semiconductor materials, the *quantum efficiency* varies, but can reach very high values over 95%. Due to noise contributions caused by thermal excitations conventional photodiodes cannot be used for the detection of single photons or light with low photon numbers, i.e. they lack single-photon sensitivity. For intense light these noise contributions can largely be neglected and for a perfect detector with $\eta = 1$ the photon current relates to the light statistics as

$$i(t) = \frac{n_e(t)e}{\Delta t},$$

where n_e is defined as the number of photo-electrons and e as the elementary charge. If we want to take into account the finite quantum efficiency η we can model the real detector by an ideal detector preceded by a beam splitter representing an effective loss of $1 - \eta$ (see e.g. [3]).

For the detection of single photons the signal of the absorbed photon has to be internally amplified to generate an electronic output which lies above the noise floor (see figure 6). This can be accomplished by avalanche photodiodes (APDs) which are designed such that in addition to an absorption region they exhibit a multiplication area. If an electron–hole pair is generated by photon absorption, a high voltage across the multiplication region causes the generation of secondary electrons. In these diodes impact ionization allows for high internal photon-current gain. For single-photon detection the APDs have to be operated in the Geiger mode where the APD is biased above its breakdown voltage. Thus, a single electron–hole pair can activate an avalanche process with an exponential growth of free carriers leading to macroscopic photocurrents. In order to prevent damage and to enable subsequent detection the avalanche has to be quenched by lowering the applied voltage. In active quenching circuits the current flow gets actively interrupted to increase the speed of resetting the APD. An APD module operated in the Geiger mode is specified by its basic properties: *quantum efficiency*, *dark count rate* and *dead time*. In the case of APDs, the quantum efficiency denotes the probability that a single photon gets recorded. A typical top value for the quantum efficiency of an APD at the wavelength regime around 700 to 800 nm is given as 60% to 70%; for wavelengths between 1200 and 1600 nm the newest generation of APDs reaches values over 25%. The dark count rate corresponds to the noise of the detector and is defined by the number of detection events in the absence of an optical signal. We have again to distinguish between APDs at 800 nm—where dark count rates as low as 100 counts per second can be easily achieved—and APDs in the telecommunication wavelength regime with dark count rates so high that active gating is essential. For a gate time of 1 ns their typical dark noise shows values between 10^{-5} to 10^{-6}. The dead time of the APDs specifies the minimum time which is needed to register consecutive detection events. For 800 nm APDs dead times as low as 50 ns are common, for APDs around 1500 nm the active gating requires dead times over 1 μs.

Figure 7 shows the output of an APD module for an optical signal with an average of more than one photon per dead time interval. Since the dead time sets a minimum time delay between detection events the repetition rate of avalanche photo-detection is restricted. The depicted output signal is provided by the electronics of the APD modules and should be understood as logic ON/OFF or 'CLICK' readout.

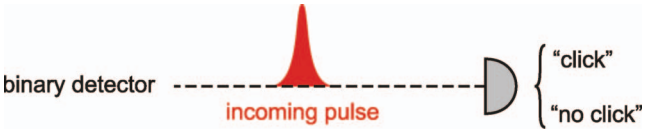

Figure 6. Avalanche photodiodes (APD) are binary detectors. They exhibit single-photon sensitivity, but can only measure if *any* light is present not how many photons are incident.

5. Detecting quantum with conventional photodiodes

5.1 *Direct detection*

For intense light standard photodiodes can serve to characterize quantum properties of light by direct detection. An important parameter for the quality of state characterization is the quantum efficiency of the detectors since it defines the accuracy of the mapping of the photon statistics onto detected distributions of photo-electrons. Because photodiodes exhibit high quantum efficiencies they are best suited to detect quantum effects which are highly

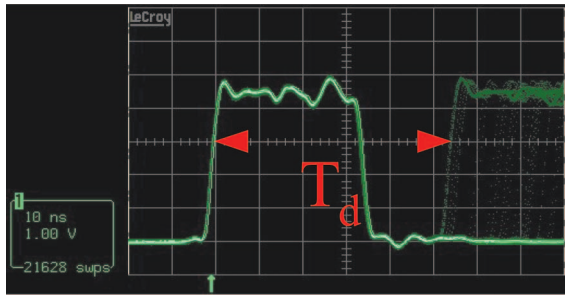

Figure 7. Typical output signal of an APD module [4], when it is operated at 'high' intensities. During the dead-time T_d no subsequent signal gets registered even though there are optical signals impinging on the diode.

sensitive to the detection efficiency, or losses, respectively. However, direct photocurrent measurements are restricted to the investigation of the amplitude quadrature, which is defined as the quadrature direction orientated along the classical displacement α (see figure 8).

For large field amplitudes the field operator $\hat{a}$ is typically decomposed into the 'classical' displacement α and the quantum operator $\delta\hat{a}$, yielding $\hat{a} = \alpha + \delta\hat{a}$. If $\alpha \gg 1$ we can employ a linearized approach and consider only the first-order terms of $\delta\alpha$. For photo-detection without reference phase we can further assume that α is real. The photon number operator then reads

$$\hat{N} = \alpha^2 + \alpha\delta\hat{X}_a,$$

which indicates that the photocurrent corresponds directly to an amplitude quadrature measurement. Hence, the properties of the amplitude quadrature can be measured by analysing the generated photocurrent $i(t) \propto \langle\hat{N}\rangle$.

5.2 *Homodyne detection*

For dark quantum states with low mean photon number, i.e. $\alpha \lesssim 1$, we can use the interference between the low intensity signal state and an intense laser beam at a beam splitter to acquire information about the signal quantum state. The setup for such measurements is depicted in figure 9; it constitutes the well-established homodyne detector. The intense reference laser beam with field amplitude $|\beta| \gg 1$ is taken as a coherent quantum field and is called a local oscillator. By applying the beam splitter relationships $\hat{c} = 2^{-1/2}(\hat{a} + \hat{b}), \hat{d} = 2^{-1/2}(\hat{a} - \hat{b})$ and calculating the photon numbers $\hat{N}_{c/d}$ at the output, we derive in the linearized approximation

$$\hat{N}_{c/d} = |\beta|^2 + \beta^*\delta\hat{b} + \beta\delta\hat{b}^\dagger \pm \beta\delta\hat{a} \pm \beta^*\delta\hat{a}^\dagger.$$

The difference of the output photocurrents is then determined by

$$\langle\hat{N}_d - \hat{N}_c\rangle \propto \beta^*\hat{a} + \beta\hat{a}^\dagger = |\beta|\langle\hat{X}^a_\phi\rangle,$$

where we use for the local oscillator the definition $\beta = |\beta|\exp(-\mathrm{i}\phi)$ and denote for the signal input state $\hat{X}^a_\phi$ as the general quadrature operator. Note that in the homodyne setup the uncertainties of the signal state get effectively amplified by the coherent field amplitude β of the local oscillator. If we assume the local oscillator to be a coherent state with $\langle\delta X^{\delta b}_\phi\rangle = 1$ we further obtain for the sum of the photocurrents

$$\langle\hat{N}_d + \hat{N}_c\rangle = \langle\beta^*\ \delta\hat{b} + \beta\ \delta\hat{b}^\dagger\rangle = |\beta|\langle\hat{X}^{\delta b}_\phi\rangle = |\beta|.$$

Thus, detecting the difference of the photocurrents yields a measurement of a general quadrature where the phase angle ϕ defines a rotation with respect to $\hat{X}$ (see figure 9). The sum of the photocurrents provides the reference such that the ratio between the sum and difference currents reflects a measurement of the normalized marginal distributions of the corresponding quadrature in the phase space.

Technically the detection of quadrature uncertainties requires one to analyse the fluctuations of the generated photocurrent $i(t) \propto \langle\hat{n}\rangle$ where a lot of experiments employ a radio frequency (rf) spectrum analyser to determine the Fourier components of the time-dependent quadrature measurements

$$\delta\hat{X}(\Omega) = \mathcal{F}\big(\delta\hat{X}(t)\big)\big|_\Omega = \int_{-\infty}^{+\infty} \delta\hat{X}(t)\ \exp\left(\mathrm{i}\Omega t\right)\mathrm{d}t.$$

The radio frequency Ω can be understood in a semi-classical approach as the frequency of the side band of an amplitude oscillation. Note that for pulsed state generation

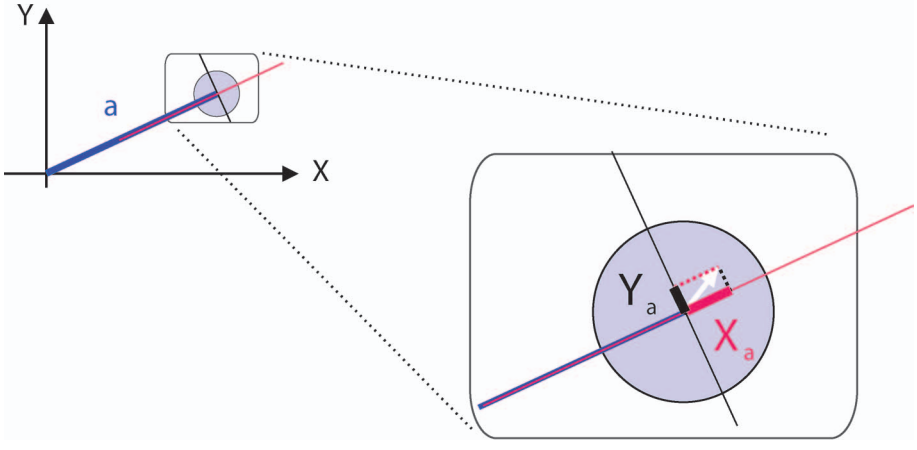

Figure 8. Amplitude X_a and phase quadrature Y_a of an intense light beam with 'classical' field amplitude α in a phase space representation.

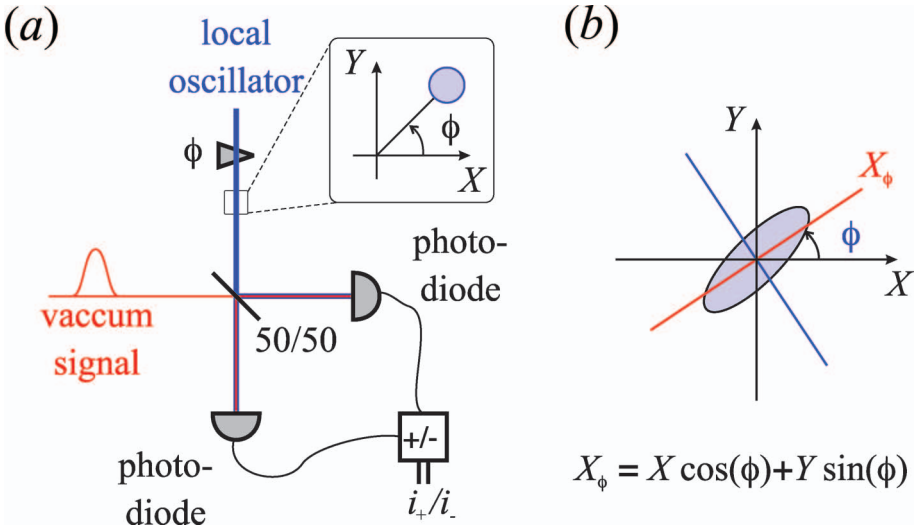

Figure 9. (*a*) Homodyne detection setup: the dark 'vacuum' signal is superimposed with a local oscillator at a symmetric beam splitter and subsequently detected with two conventional photodiodes. (*b*) The sum and difference currents yield information about the marginal quadrature corresponding to the angle ϕ (see text).

rf detection schemes imply an averaging over several pulses hindering single-shot resolved detection. Time-resolved homodyne detection employs different electronics to integrate the photocurrent over the duration of one light pulse, such that single-shot measurements of the quadrature operator become possible [5–9].

Homodyne detection allows one to measure phase sensitive properties of light and can indeed be used to reconstruct the Wigner function of the state by tomographic reconstruction [10]. Since there exists a unique mapping between the Wigner function of a state and its density matrix, the method of homodyne tomography is suited for the complete state characterization. Once the density matrix of a state is known, we can also assess the photon statistics which are given as diagonal elements of the matrix [11]. The homodyne detection technique was first demonstrated by Smithey *et al.* in 1993 [8]. Since then the virtue of homodyning has been proven in a multitude of experiments (for review see [12]) and can be explained by the possibility to utilize standard photodiodes which can exhibit very high quantum efficiencies.

Nevertheless, the method of homodyning implies a few drawbacks one should be aware of, especially if we are mainly interested in the photon statistics of the signal. First of all the tomographic reconstruction is only an indirect ascertainment of the photon statistics, which requires a laborious series of measurements. Secondly, the usage of a local oscillator is inevitable which in turn implies that the mode of the local oscillator has to be perfectly matched with the signal state. This impacts the state characterization twofold: every mode mismatch has the same characteristic as loss such that it is hard to give a good estimate of the efficiency of the detection. Furthermore, the need for a local oscillator also entails an intrinsic filter operation, since only the part of the signal which overlaps spatially and spectrally with the local oscillator mode gets amplified by the interference and subsequently detected by the photodiodes. In current research homodyne detection is an essential tool for continuous variable quantum communication systems [13], which employ a pair of conjugate quadratures to encode information. However, it has been shown recently [14] that more complex communication networks based on continuous variable states require necessarily to combine homodyning with some type of avalanche photo-detection to counteract decoherence effects of quantum channels by so-called entanglement distillation. This task can be accomplished by preparing photonic states with non-Gaussian Wigner functions by conditioning on APD detection events [15–17]. For these states a more elaborated theoretical description, which takes into account the spectral and spatial properties of the light, is needed to study the impact conditional state preparation in combination with homodyne detection [18].

6. Avalanche photo-detection

While APDs exhibit single-photon sensitivity they cannot distinguish between different photon numbers. They deliver binary outcomes 'CLICK' and 'NO CLICK', which indicate whether any light was incident or not, but a photon number resolved detection remains difficult. Thus, the question arises how much information can be gained with a single APD.

For a single photon with exact photon number $n = 1$, the probability that an APD records a 'CLICK' event is given by the associated quantum efficiency η, and likewise the probability of 'NO CLICK' is $1 - \eta$. If n photons are impinging on the APD, they will only *not* cause an avalanche process if all of them get lost and thus do not generate an initializing electron–hole pair. Hence, the probability of the 'NO CLICK' event for a quantum state with exactly n photons is given by $(1 - \eta)^n$ and the corresponding measurement operator reads

$$\hat{M}_{\text{'NO CLICK'}} = \sum_{N=0}^{\infty} (1 - N)^N |N\rangle\langle N|.$$

Since the probabilities of outcomes 'CLICK' and 'NO CLICK' have to add up to one, i.e. in terms of measurement operators they sum up to the unity operator $\mathbb{1}$, the measurement operator of an APD is given by

$$\hat{M}_{\text{APD}} = \mathbb{1} - \hat{M}_{\text{'NO CLICK'}}.$$

To find the probability of an APD 'CLICK' for a general quantum state $\hat{\rho} = \sum_{m,n} c_{mn} |n\rangle\langle m|$ we can calculate in analogy to the photon counting probabilities

$$p_{\text{'CLICK'}} = 1 - \text{tr}\left(\hat{\rho}\hat{M}_{\text{APD}}\right) = \sum_n c_{nn}(1 - \eta)^n,$$

where the diagonal elements c_{nn} of the density matrix denote the probability of a n-photon number contribution.

The derived formula indicates that the binary APD response actually contains some information about the impinging photon numbers if different efficiencies are taken into account. The efficiency can be artificially modified by introducing a well-defined loss in front of the APD, i.e. performing attenuation measurements with a beam splitter with variable calibrated transmission coefficient η_t. A n-photon number state $|n\rangle$ will then show an attenuation behaviour corresponding to the function $(1 - \eta_t)^n$ and different photon number can principally be distinguished in ensemble measurements if APD 'CLICK' statistics are recorded for various values of η_t. For general photonic states a complete reconstruction of the photon-number statistics can be feasible if sufficient data with various η_t is recorded [19,20].

Contrariwise, if we want to test the validity of the APD modelling with the described measurement operators we need to control the influence of the photon statistics precisely. To do so, we can utilize attenuated coherent light which is known to exhibit Poissonian statistics (see above). Describing the variable attenuation as a beam splitter with transmission parameter η_t we find that for coherent states only the mean field amplitude is lowered to a value of $\eta_t \cdot \alpha$, whereas all higher moments remain unchanged, i.e.

$$|\alpha\rangle \rightarrow |\eta_t\alpha\rangle = \exp\left(-\frac{|\eta_t\alpha|^2}{2}\right) \sum_n \frac{(\eta_t\alpha)^n}{(n!)^{1/2}} |n\rangle.$$

For the probability of an APD 'CLICK' we obtain

$$p_{\text{'CLICK'}} = 1 - \exp\left(-|\eta_t\alpha|^2\right).$$

Thus, we can conclude that for very low intensities of the laser light $\alpha < 1$, the rate of APD counts shows a linear dependency on the attenuation factor as expected from the scaling of the light intensity as well as for single-photon states. Though for higher intensities we find a nonlinear response indicating the saturation of the APDs which is caused by multi-photon contributions. The exponential dependency of APD rates can be nicely demonstrated experimentally by setting up an experiment with appropriate calibrated loss (see figure 10); note, however, that the measurement of the absolute field amplitude α for small alpha is difficult, because the effective value detection efficiency η_t is typically not very well calibrated.

The dead time of the avalanche process imposes another limitation on APD detection, which restricts ultimately the maximum speed of possible data acquisition. For cw light APD modules are specified that they can only accept count rates up to a Mcounts s^{-1}, such that it seems that a maximum repetition rate of 1 MHz is possible for pulsed systems. However, the dead times of the actively quenched APD modules is specified to lie around 50 ns, which corresponds a to repetition rate of 20 MHz. This discrepancy can be understood if one considers the impact of dead time for increasing intensities. If an APD records a detection event, it cannot detect a second event within the

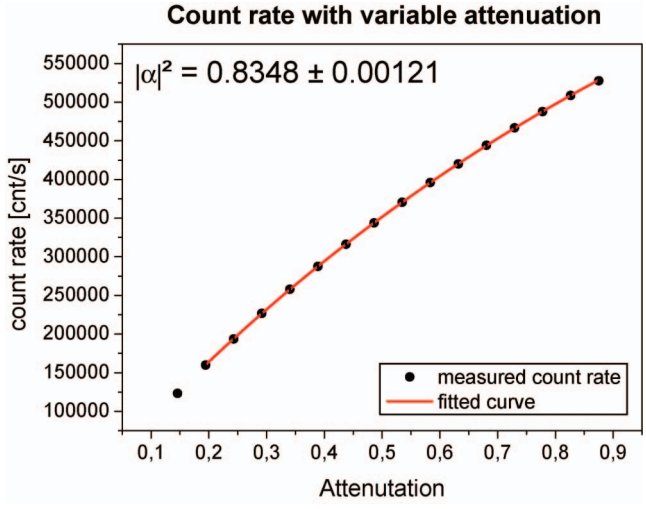

Figure 10. APD detection: influence of multi-photon contributions [21]. APD detection rates for laser light with variable attenuation shows a nonlinear response according to the expected exponential behaviour. The nonlinearity can be attributed to multi-photon contributions of the Poissonian statistics [21].

dead time, i.e. it is effectively blocked during this time period. This APD operation is illustrated in figure 11.

For cw light possible detection events are randomly distributed over time, such that with increasing intensities the probability that a second event following an APD 'CLICK' becomes more and more likely. In this situation a noticeable difference between expected and measured count rates can be observed for rates above 1 MHz. Conversely, for pulsed systems we can ensure that there is no possible detection event during the dead time by adjusting the repetition rate accordingly. In this situation we can show for sufficiently low α that up to a repetition rate $f_{\mathrm{rep}}^{\max} = 1/T_{\mathrm{D}}$ a linear response is recorded, and a step-shaped fall-off of the count rates around $f_{\mathrm{rep}}^{\max}$ indicates that the APD are ready for another APD event with the same detection efficiency shortly after the dead time [21].

7. Photon number resolved detection

Up to very recently no practical photon-number resolving (PNR) detectors were available. Thus, most of the previous experimental work in the field for characterizing properties of multi-photon states with low mean photon numbers is based on homodyne detection schemes. To date there exists various approaches to realize PNR detectors utilizing different methods. As benchmarks one can specify the characteristics of *quantum efficiency*, *dark counts*, *operating temperature* and possible *time resolution*.

One of the first attempts to accomplish the direct detection of photon statistics was performed in 1982 with a photo-multiplier tube [22]. Though the time resolution can be pretty high, the main drawback of this detection is a comparatively low quantum efficiency $<20\%$, such that a good mapping between impinging and detected photon statistics is not provided. In more recent developments

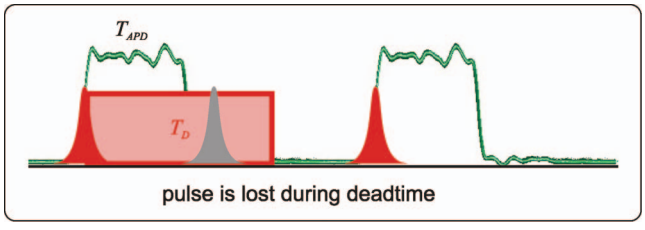

Figure 11. APD detection: influence of dead time. After a detection event (depicted as read pulse) with corresponding electronic signal T_{APD} (green curve) the APD is not ready for registering a second event during the dead time T_{d} (indicated by the red region). Possible detection events (grey pulse) during this time period get lost in the recorded signal; pulses immediately following the dead time (green pulse) are again detected (figure: courtesy: H. Coldenstrodt-Ronge).

superconducting devices, such as transition edge transistors or balometers [23–27], have been investigated. They have high quantum efficiencies and comparatively low dark count noise, but require cryogenic cooling devices in order to achieve the extremely low operating temperatures. A promising development is the 'visible light photon counter' (VLPC) offering extraordinarily high quantum efficiencies around 90%, but it lacks a low dark noise level and again relies on cryogenic cooling [28].

As an alternative one can apply a multiplexed detection scheme utilizing binary APDs for the actual detection itself. In this approach the signal input light gets probabilistically split into a sufficiently large number of output modes by optical means in front of the binary detectors, which themselves are not capable of resolving photon numbers, but exhibit single-photon sensitivity. The probability of two or more photons of staying together and ending up in the same mode—such that they do not get registered as two or accordingly more—scales with the number of output modes. For example, for two photons the probability that they will not be seen as two is given by $1/N$, where N is the number of output modes. The detected 'CLICK' statistics reflect a good measurement of the input photon statistics. The quality of this type of PNR detectors depends crucially on N, which means we need a multiplexing of the input modes which is adopted to the number of expected input photon numbers. The first suggestion to implement this idea experimentally was presented 1996 by Paul *et al*. [29] and later analysed in more detail [30], where it is proposed to utilize a beam splitter cascade followed by N APDs. A scheme of such a setup is shown in figure 12. The first beam splitter divides the input light into two beams, where each of them is again subdivided into two parts. By repeating the described procedure an arbitrary number of output modes can be obtained in principle, but unfortunately the experimental complexity and the number of required APDs scales accordingly.

To circumvent the difficulties of spatial multiplexing Banaszek and Walmsley suggested and characterized in 2003 a scheme which implements the 'photon-chopping' for pulsed light by using temporal modes instead of spatial ones [31]. Though their layout still employed a fast optical switch in combination a fibre loop. The active optical switch was required to find a good compromise between a high transmission for coupling the signal light into the loop and a low transmission for the output coupling for the pulses prepared for 'CLICK' detection. A more elaborate setup, which is also based upon time-multiplexing and fibre networks, but does not necessitate active optical elements was presented in 2003 independently by Achilles *et al*. [32] and Fitch *et al*. [33]. Their time-multiplexing detector (TMD) utilizes two spatial modes and an 'arbitrary' number of temporal modes. In its simplest form (see figure 13) it consists of three 50:50 beam splitters and fibre loops of

variable lengths, such that at the output of the fibre system input pulses are split into two times four temporal modes (see figure 14). In contrast to a typical beam splitter cascaded system the outputs of one beam splitter stage in the cascade are not left separated but recombined on the beam splitter of the next stage. A time delay is properly chosen and introduced into one of the arms before combining the two signal paths again, such that the APD signals resulting from earlier modes do not overlap and disturb each other within their dead times. This setup can be extended with subsequent stages to achieve 2^k (k being the number of stages) modes.

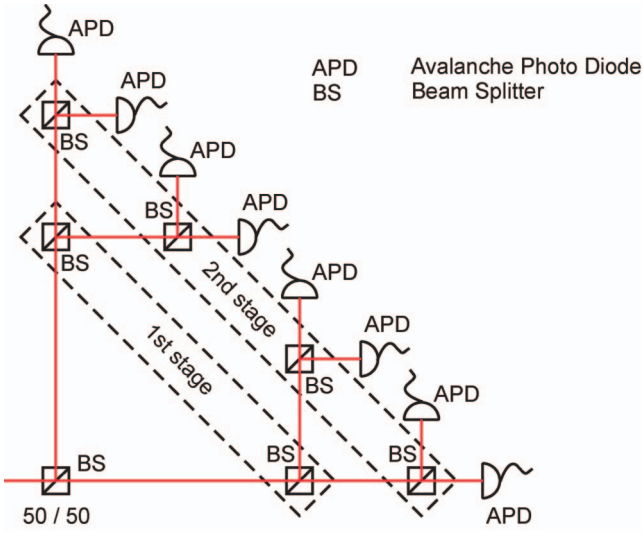

Figure 12. Multiplexed detection scheme: the input light is divided into eight output modes which are subsequently detected by binary APD measurements. In this scheme each stage needed for doubling the modes requires a 2^k beam splitter, where k labels the numbering of the stages (see figure); the detection is carried out by N APDs. The click statistics represent the photon statistics of the input mode provided the number of outgoing modes is much larger than the expected photon numbers of the input light.

For states with low enough mean photon numbers the count statistics will indicate the photon number distribution of the input quantum state, but not directly match it. Their are two 'flaws', which have to be considered. First of all, we know that the detection efficiency of the APDs does not reach close to unity and furthermore, the fibre network also introduces additional losses. Secondly, although the effect of photons not being separated by the fibre network can always be suppressed by a larger number of modes N, this reduces the allowed repetition rates, i.e. the speed of the detection.

For quantum state characterization, i.e. in ensemble measurements, one can nevertheless show that the photon number statistics can be reconstructed from the count statistics and the involved convolution can actually be treated independent of the losses [34]. The probability P_k of detected 'CLICK' statistics is linked to the signal photon number distribution p_n by

$$P_k = \sum_n p_{kn}(k|n)p_n,$$

where $p_{kn}(k|n)$ denotes the conditional probability of obtaining k 'CLICK's if the observed photon number of the

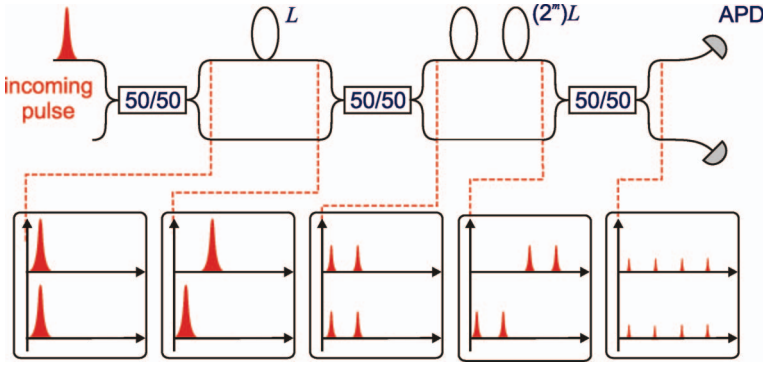

Figure 13. Time-multiplexed detector (TMD): the beam splitter cascade for dividing the input light into a sufficiently large number of output modes is realized in a time-multiplexed scheme which utilizes only passive linear elements. The time multiplexing is accomplished by two spatial modes and in this case four temporal modes. After the first beam splitter the pulsed input light is separated into two spatial modes and a fibre loop in the upper mode introduces a delay of the corresponding pulse. At the next beam splitter—now corresponding to the first stage of figure 12—the delayed pulse and the pulse from the lower arm do not interfere with each other resulting into a division into $2 \times 2 = 4$ modes. Each iteration of this step leads to a doubling of the previous mode number, i.e. after k stages one can generate 2×2^k output modes for subsequent detection realized by 2 APDs.

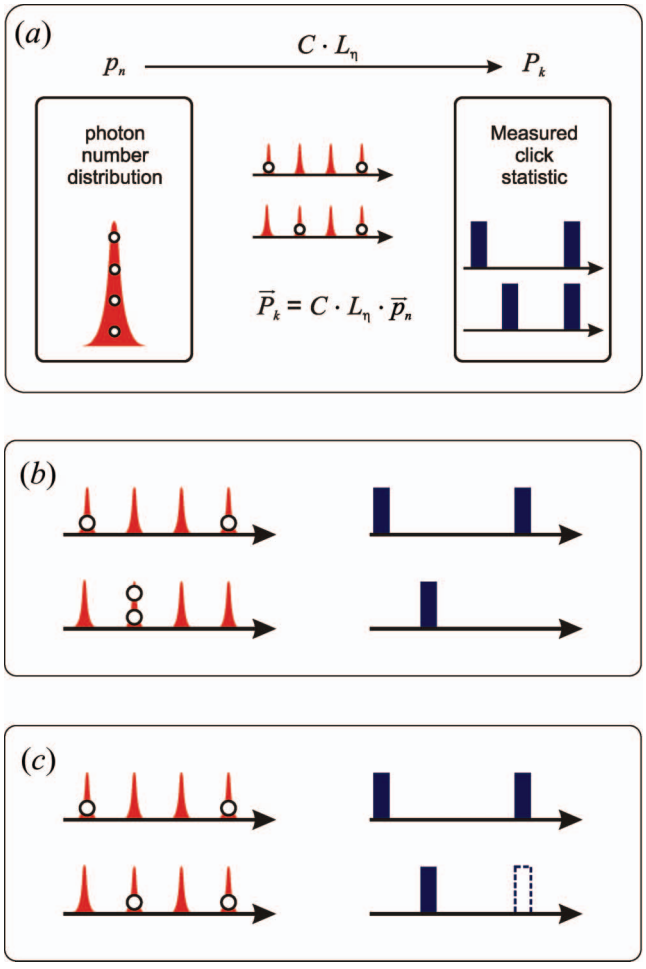

Figure 14. Modelling of the time-multiplexed detector (TMD): (*a*) ideally the click statistics reflect directly the incident photon statistics of the input pulse. The four input photons get distributed into different time slots by the network and can get detected by APDs; the theoretical modelling requires to include convolution and loss effects, but there exists a deterministic matrix relationship between 'CLICK' statistics and the photon statistics. (*b*) and (*c*) Imperfections of TMD detection: (*b*) due to the statistical nature of the splitting in the network exists a finite probability that two photons stick together in one pulse and the 'CLICK' count a too small photon number; in the matrix relationship this can be taken into account by the convolution matrix C: (*c*) some photons can get lost during detection; the loss matrix L accounts for this in the theoretical description.

quantum measurement corresponds to p_n. In a matrix representation the same equation can be written as

$$\mathbf{P}_k = C \cdot L_\eta \mathbf{p}_n,$$

where we now introduced the probability vectors $\mathbf{P}_k = (P_k)$ and $\mathbf{p}_n = (p_n)$ and the matrices C and L_η reflect the convolution and loss imperfections, respectively. It can be shown that treating these two effects independently one after the other is justified by lumping all losses in front of the detector and considering it as an effective overall loss [35]. The loss matrix is given by

$$L_{kn} = \binom{n}{k} \eta^k (1-\eta)^{n-k}$$

defining $\binom{n}{k} = 0$ for $n < k$. If we assume an idealized TMD with absolutely symmetric splitting we obtain for the convolution matrix the form [29]

$$C_{kn} = \binom{N}{k} \sum_{i=0}^{k} \binom{k}{i} (-1)^i \left(\frac{k-i}{N}\right)^n.$$

Note that in this approach there exists a deterministic relationship between the observed 'CLICK' statistics and the actual signal photon number distribution of the input light. Thus, after measuring a sufficiently large collection of equivalently prepared signal states†; we can determine the corresponding frequencies of the number of 'CLICK' to obtain a good estimate of measured probabilities P_k. This allows us to invert the described matrix relationship between the photon number and 'CLICK' statistics. Provided that the parameter η is well known, the original statistics of the incident photon numbers can be acquired. In contrast to typical homodyning detection in such measurements losses and/or mode overlap considerations do not play any role anymore. Though, similar to judging the loss calibration for APD measurements, it is difficult to evaluate the loss parameter η with sufficient accuracy for the relevant quantum states with very low mean photon number. Still, with the described inversion method it becomes possible to accomplish loss-tolerant characterization of photon number statistics, if we employ *a priori* information about the source of the signal states [36]. This allows us to study quantum properties of light with an alternative approach which encounters other experimental imperfections other than homodyne tomography.

For the complete characterization of quantum light the determination of photon statistics is not sufficient, since the phase relationships between the different photon number contributions is not determined, i.e. the phase of the complex coefficient c_n in the state description $|\Psi\rangle = \sum_n c_n |n\rangle$ or equivalently the offdiagonal components c_{mn} in the density matrix representation $\hat{\rho} = \sum_{m,n} c_{mn} |m\rangle\langle n|$ are not fixed. Thus, we need an additional reference beam,

†We would like to stress that for state characterization it is always implicitly assumed that a large sample of identical signal states is prepared and measured, because a single measurement outcome does not render any information about probability distributions, which are necessary for quantum state characterization.

as done in homodyning, to establish a thorough quantum state characterization utilizing direct detection of photon statistics. In this context, it has been shown, however, that the Wigner function at the origin $\alpha = 0$, i.e. $X = 0$ and $Y = 0$, can be directly related to photon statistics by evaluating the parity of the state [37], i.e.

$$W(0) = \frac{2}{\pi}\sum_n (-1)^n \langle n|\hat{\rho}|n\rangle = \sum_n (-1)^n p_n.$$

If we now apply the displacement operator $\hat{D}(\alpha) = \exp(\alpha\hat{a}^\dagger - \alpha^*\hat{\alpha})$ to the signal state and probe the parity of the photon statistics, we sample effectively the Wigner function at the displaced value α by

$$W(\alpha) = \sum_n (-1)^n \langle n|\hat{D}(\alpha)\hat{\rho}\hat{D}^\dagger(\alpha)|n\rangle.$$

For the implementation of the displacement the signal state has to be overlapped with a strong reference beam at a highly asymmetric beam splitter with high transmission.

Traditionally we are used to characterizing multi-photon states by homodyne detection in phase space and determining photon statistics in ensemble measurement by tomographic means. For conditional preparation homodyne measurement results can only be used to select specific states based on quadrature measurements such that conditioning on a specific photon number—needed for the preparation of non-Gaussian states—is intrinsically impossible. Contrariwise, we can also accomplish complete state characterization in the photon number basis by using photon number resolving detectors. Each single measurement result for a single shot measurement corresponds to measurements of photon statistics which offers the possibility of preparing more sophisticated quantum states. Ensemble measurements for different photon numbers can be used vice versa to determine the complete Wigner function in phase space where in contrast to homodyne detection we sample the Wigner function point by point defined by the applied displacement. Further studies between the different detection approaches can be expected to give us a deeper understanding for quantum state characterization, preparation and manipulation in general.

8. Conclusion

The detection of genuine quantum characteristics of light can be carried out by different methods where the properties of detectors themselves play a major role how we describe the quantum light. Traditionally most of the interest has been devoted to homodyne detection to study multi-photon states. Otherwise APD measurements have been used to analyse single photon states, where it is mostly assumed that higher photon number contributions can be neglected such that APD detection is adequate. Current research now focuses on more advanced multi-photon states with non-Gaussian Wigner functions and alternative routes for characterizing light be detecting photon statistics. This in turn stimulates the development of new detector concepts and more elaborate theoretical treatment, which include all characteristics of the considered fields. These developments provide us with the distinct approaches for quantum state metrology which are likely to prove fruitful for various applications in quantum enhanced technology.

References

[1] L. Mandel and E. Wolf, *Optical Coherence and Quantum Optics* (Cambridge University Press, Cambridge, 1995).
[2] G. Leuchs, Contemp. Phys. **29** 299 (1988).
[3] S. Barnett and P. Radmore, *Methods in Theoretical Quantum Optics* (Oxford University Press, Oxford, 2003).
[4] *SPCM-AQR Single Photon Counting Module Datasheet* (PerkinElmer Inc., Vaudreuil, QC, Canada, 2005).
[5] A. Zavatta, M. Bellini, P.L. Ramazza, *et al*., J. Opt. Soc. Am. B **19** 1189 (2002).
[6] H. Hansen, T. Aichele, C. Hettich, *et al*., Opt. Lett. **26** 1714 (2001).
[7] M.G. Raymer, J. Cooper, H.J. Carmichael, *et al*., J. Opt. Soc. Am. B **12** 1801 (1995).
[8] D.T. Smithey, M. Beck, M.G. Raymer, *et al*., Phys. Rev. Lett. **70** 1244 (1993).
[9] J. Wenger, R. Tualle-Brouri and P. Grangier, Opt. Lett. **29** 1267 (2004).
[10] U. Leonhardt, *Measuring the Quantum State of Light* (Cambridge University Press, Cambridge, 1997).
[11] G. Breitenbach, S. Schiller and J. Mlynek, Nature **387** 471 (1997).
[12] A.I. Lvovsky and M.G. Raymer, arXiv:quant-ph/0511044 (2005).
[13] S.L. Braunstein and P. van Loock, Rev. Mod. Phys. **77** 513 (2005).
[14] J. Eisert, S. Scheel and M.B. Plenio, Phys. Rev. Lett. **89** 137903 (2002).
[15] J.S. Neergaard-Nielsen, B. Melholt Nielsen, C. Hettich, *et al*., Phys. Rev. Lett. **97** 083604 (2006).
[16] A. Ourjoumtsev, R. Tualle-Brouri, J. Laurat, *et al*., Science **312** 83 (2006).
[17] K. Wakui, H. Takahashi, A. Furusawa, *et al*., arXiv:quant-ph/0609153 (2006).
[18] P. Rohde, W. Mauerer and Ch. Silberhorn, New. J. Phys. **9** 91 (2007).
[19] J. Wenger, J. Fiurasek, R. Tualle-Brouri, *et al*., Phys. Rev. A **70** 053812 (2004).
[20] G. Zambra, A. Andreoni, M. Bondani, *et al*., Phys. Rev. Lett. **95** 063602 (2005).
[21] H. Coldenstrodt-Ronge and C. Silberhorn, J. Phys. B: At. Mol. Opt. Phys. **40** 3909 (2007).
[22] R.S. Bondurant, P. Kumar, J.H. Shapiro, *et al*., Opt. Lett. **7** 529 (1982).
[23] B. Cabrera, R.M. Clarke, P. Colling, *et al*., Appl. Phys. Lett. **73** 735 (1998).
[24] M. Fujiwara and M. Sasaki, Opt. Lett. **31** 691 (2006).
[25] R.H. Hadfield, M.J. Stevens, S.S. Gruber, *et al*., Opt. Exp. **13** 10846 (2005).
[26] D. Rosenberg, A.E. Lita, A.J. Miller, *et al*., Phys. Rev. A **72** 019901 (2005).
[27] S. Somani, S. Kasapi, K. Wilsher, *et al*., J. Vac. Sci. Technol. B **19** 2766 (2001).
[28] J.S. Kim, S. Takeuchi, Y. Yamamoto, *et al*., Appl. Phys. Lett. **74** 902 (1999).
[29] H. Paul, P. Torma, T. Kiss, *et al*., Phys. Rev. Lett. **76** 2464 (1996).
[30] P. Kok and S.L. Braunstein, Phys. Rev. A **63** 033812 (2001).
[31] K. Banaszek and I.A. Walmsley, Opt. Lett. **28** 52 (2003).

[32] D. Achilles, C. Silberhorn, C. Sliwa, *et al*., Opt. Lett. **28** 2387 (2003).
[33] M.J. Fitch, B.C. Jacobs, T.B. Pittman, *et al*., Phys. Rev. A **68** 043814 (2003).
[34] D. Achilles, C. Silberhorn, C. Sliwa, *et al*., J. Mod. Opt. **51** 1499 (2004).
[35] C. Silberhorn, D. Achilles, A.B. U'Ren, *et al*., presented at Proceedings of the Seventh International Conference on Quantum Communication, Measurement and Computing QCMC 2004, Glasgow, UK, 25–29 July (2004).
[36] D. Achilles, C. Silberhorn and I.A. Walmsley, Phys. Rev. Lett. **97** 043602 (2006).
[37] K. Banaszek and K. Wodkiewicz, Phys. Rev. Lett. **76** 4344 (1996).

Christine Silberhorn studied physics and mathematics at the Friedrich-Alexander University of Erlangen, Germany and received her PhD in 2003 working on continuous variable quantum systems. In the same year she moved to Oxford and became a post-doctoral reasearch assistant at the Clarendon Laboratory, Oxford University where she started research in the field of discrete variable quantum states. Since 2005 she has been heading an Independent Junior Research Group at the Max Planck Research Group for Optics, Information and Photonics at Erlangen.